Journal of Food Bioactives
International Society for Nutraceuticals and Functional Foods
Original Research
J. Food Bioact. 2026;34:65–74

Nanoparticles of kaempferol loaded in deamidated zein/pectin protein: Formation, stability, improved antioxidant capacity, and enhanced bioaccessibility

Xiaoyun Rong[a], Jiandong Ren[b], Chao Huang[a], Xinbo Guo[c], Fenglin Song[a], Yongguang Bi[d,e], Kun Hu[a*] and Ruixue Guo[a*]

[a]Department of Food Science, Guangdong Pharmaceutical University, Guangzhou 510006, China
[b]Department of Food Science and biotechnology, Guangdong University of Education, Guangzhou, 510006 China
[c]School of Food Science and Engineering, South China University of Technology, Guangzhou 510640, China
[d]Department of Pharmacy, Guangdong Pharmaceutical University, Guangzhou 510006, China
[e]Guangdong Dongshenglin Pharmaceutical Co., Ltd, China
[*]**Corresponding author:** Kun Hu and Ruixue Guo, Department of Food Science, Guangdong Pharmaceutical University, Guangzhou, 510006, China. E-mail: China. huk@gdpu.edu.cn (KH), cindygrx@163.com (RG)
DOI: 10.26599/JFB.2026.95034449
Received: March 21, 2026; **Revised received & accepted:** May 13, 2026
Citation: Rong, X., Ren, J., Huang, C., Guo, X., Song, F., Bi, Y., Hu, K., and Guo, R. (2026). Nanoparticles of kaempferol loaded in deamidated zein/pectin protein: Formation, stability, improved antioxidant capacity, and enhanced bioaccessibility. J. Food Bioact. 34: 65–74.

Abstract

Kaempferol is a dietary polyphenol with abundant bioactivities such as anti-inflammatory, antioxidant and anticancer. However, its poor bioavailability limits the utilization. Therefore, food-grade delivery formulations are explored to overcome it. In this study, kaempferol was loaded into deamidated zein/pectin to prepare complex nanoparticles (KZN) with a diameter of 158.3 nm and loading efficiency of 89.54%. The kaempferol exists in amorphous form within the complex nanoparticles. Fourier transform infrared spectroscopy suggested hydrogen bonding and electrostatic interactions were the main force holding these complexes together. Heating, sodium chloride addition and pH changes did not result in aggregation of KZN. Compared with free kaempferol, the bioaccessibility of kaempferol complexed with zein nanoparticle was enhanced 2-fold, which attributed to higher antioxidant activities. Overall, this study indicates that the KZN had great potential as a delivery technique for hydrophobic compounds in nutraceutical and pharmaceutical applications.

Keywords: Kaempferol; Deamidation; Zein nanoparticles; Bioaccessibility; Antioxidant capacity.

1. Introduction

Kaempferol (3, 5, 7, 4′-tetrahydroxylflavone) is a natural flavonol that has been found in 80% of plant-based foods like broccoli, leafy vegetables, tomato, beans, berries, apples, saffron, tea, etc (Chen and Chen, 2013; Imran et al., 2019). Recently, plant-derived bioactive compounds, as kaempferol, becomes a popular research topic due to their various bioactivities such as anti-inflammatory, anticancer, antioxidant, antidiabetic, antibacterial, antimicrobial and cardiovascular protective effects and their high biocompatibility and lack of side effects, in comparison with synthetic drugs (Chen and Chen, 2013; Imran et al., 2019; Kashyap et al., 2017; Rajendran et al., 2014; Wang et al., 2019). Unfortunately, most of the natural biologically active compounds are highly unstable to high temperatures (during cooking) and oxidation. Besides, the low abundance in daily foods and low water solubility hinder the use of these compounds as functional foods or nutraceutical ingredients. Kaempferol also performed excellent protective capacity against oxidative stress in brain, and neuro-inflammation. It also has been shown to possess diverse pharmacological effects, such as antibacterial activity, anti-tumor potency and cardioprotective activities. Accumulating investigations have expounded that kaempferol exhibits significant

improvements in cardiovascular disease management, which is attributed to its role in inhibiting oxidation, inflammation, apoptosis and fibrosis. Due to its poorly water solubility, kaempferol could not easily pass through blood-brain barrier (BBB) (Silva dos Santos et al., 2021). Nanoparticles have been widely used as delivery system to increase solubility and bioaccessibility of natural active compounds (Li et al., 2015). Kaffash et al. (2024) reported an oil-in-water Nano-kaempferol formulation using tween 80 as surfactants with human serum albumin and holo-transferrin as the binary and ternary systems could significantly reduce the cell viability of the adeno-carcinoma cells of the colon SW480 via PI3K/AKT/m-TOR pathway. Combretastatin and kaempferol in the form of nanoparticles with high water solubility could attenuate angiogenesis by suppressing the activation of endothelial cells and production of cytokines promoting proliferation of cancer cells. Interestingly, the complexed nanoparticle of kaempferol and combretastatin showed better effects than kaempferol or combretastatin alone (Subbaraj et al., 2023). Solid lipid nanoparticles (SLNs) (Ghosh et al., 2024) formulated with stearic acid and polysorbate 80 were an efficient carrier for kaempferol with a mean particle size of 451.2 nm and enhanced efficiency to cross BBB. Although these reported delivery systems improved relevant bioactivity and bioavailability of kaempferol, the preparation methods were complex, or the surfactants or organic solvents is not so safe and appreciated in functional foods or nutraceuticals, that novel food-grade approaches to significantly enhance the in vivo absorption should be developed.

Zein is the most abundant storage protein in corn with great potential to be used in food industry as it is renewable and biocompatible. Moreover, zein has unique hydrophobic/hydrophilic properties, and is a promising biopolymer in the food and nutrition fields. Therefore, zein nanoparticles as food colorants, nutritional supplements, antibacterial agents, natural antioxidants and other active ingredients carrier has been widely studied by researchers (Kasaai, 2018; Zhang et al., 2016). However, there are still some defects as carrier materials, such as low sealing rate, poor water solubility, poor stability and poor dispersion after freeze-drying, these adverse factors make it limited in practical applications (Wang et al., 2024a; Türker, 2025). The glutamine and asparagine residues of zein will be cleaved by acids or base to release glutamic and aspartic amino acids. This reaction is called deamidation which will expose the inner hydrophobic core of zein protein (Cabra et al., 2007). The deamidated zein protein and hydrophobic nutrients can form nano-complex spontaneously in aqueous solutions due to hydrophobic interaction (Li and Yao, 2020).

Pectin, a negatively charged polysaccharide, can attenuate the aggregation of zein nanoparticles within aqueous solutions due to ionic interaction with carboxyl groups of zein protein (Liang et al., 2021). After alkali deamidation modification of zein, its isoelectric point decreases (Wang et al., 2024b). When the system pH is lower than the isoelectric point (PI), the protein carries a positive charge; otherwise, it is negatively charged. If both are negatively charged, the main interactions between deamidated zein and pectin are hydrogen bonding, hydrophobic interactions, and steric hindrance (Qu et al., 2024). At present, no one has used polysaccharides as stabilizers to prepare hydrophobic nutrient-loaded deamidated zein nanoparticles.

This study was aimed to formulate and study a novel food-grade delivery system with modified zein protein to encapsulate kaempferol, a hydrophobic dietary polyphenol, and to improve its bioavailability. Meanwhile, pectin was employed and adsorbed onto the surface of nanoparticles through hydrogen bonding and steric hindrance of pectin molecules, thereby inhibiting the aggregation of nanoparticles in aqueous solution. Experiments were designed and performed to investigate the formation process and properties of zein-kaempferol nanoparticles, the release kaempferol using a simulated gastrointestinal (GI) tract system, as well as the antioxidant activities of digested kaempferol-zein nanoparticles.

2. Materials and methods

2.1. Materials

Kaempferol (J1925080, 97%) was purchased from Aladdin (Shanghai, China). Zein (A0422917) and Trolox (A0405014, 97%) were purchased from Acros Organics (New Jersey, USA). 2,2′-Azinobis (ABTS) was obtained from Tokyo Chemical Industry Co., Ltd. (TCI) (TOKYO, JAPAN). L (+)-Ascorbic acid (99%) was obtained from Innochem Ltd (Beijing, China). Pectin (SLBV5461), 2,2′-azobis (ABAP, 97%), 1,1-diphenyl-2-picrylhydrazyl free radical (DPPH,>97.0%), pepsin (P6887), bile Salts, fluorescein(Lot BCBV5681) and pancreatin (P7545) were obtained from Sigma-Aldrich (St Louis, MO, USA). Other chemicals used in this study were ACS grade.

2.2. Preparation of kaempferol-loaded composite nanoparticles.

Zein was adequately dispersed into 0.5 M NaOH solution at pH of 12. After magnetically stirred (600 rpm) overnight at room temperature (24 ºC), a deamidated zein dispersion at mass fraction of 1% (w/v) was obtained. Then the temperature of such zein dispersion was increased to 70 °C and maintained for another 10 h. After that the sample was transferred to an ice bath, dialyzed for 24 h. The obtained samples are then frozen and freeze dried.

The zein-kaempferol nanoparticle was prepared according to Zhang et al. (2021) with minor modifications (Zhang et al., 2021). Briefly, 0.4g of deamidated zein was dispersed in 20.0mL of 70% (v/v) ethanol aqueous solution using a magnetic stirrer at 600rpm for 60min, then kaempferol was added and stirred for another 60min without light. After that, 4mL of kaempferol-zein solution was mixed with 16mL of pectin solution (0.1%, w/v) stirred at 800rpm for 60min. The ethanol in the solution was then removed by using a rotary evaporator (RE-2000A, Yarong, Shanghai, China) at 40 °C. Deionized water was then added to reach a final volume of 20.0 mL. The solution was freeze dried (Beta 1–8 LSC basic, CHRIST, German) to obtain zein-kaempferol nanoparticle for further experiments. Zein nanoparticles without kaempferol were also prepared following the above procedures.

2.3. Characterization of nanoparticle

2.3.1. Size measurements

The mean particle diameter (Z-average), polydispersity index (PDI), and surface potential (ζ-potential) of the nanoparticles were analyzed by using a combined dynamic light scattering/electrophoresis instrument (Nano-ZS 90, Malvern Instruments, UK) following instructions as reported (Tian et al., 2019).

2.3.2. Scanning electron microscopy

Scanning electron microscope (S-4800, Hitachi Co., Japan) was used to analyze the morphology of nanoparticles following the procedures of the instrument manual.

2.3.3. X-ray diffraction (XRD) analysis

X-ray diffraction was used to analyze the physical properties of freeze dried kaempferol nanoparticles, kaempferol/deamidated zein/pectin mixtures, pure kaempferol, pure deamidated zein and pure pectin, following previous report with slightly modification (Hu and McClements, 2014). Briefly, a Cu Kα radiation source was employed at 40 kV and 30 mA, with a scanning step of 0.02° and scanning speed of 10°/min.

2.3.4. Fourier Transform Infrared (FTIR) analysis

The freeze-dried powder of deamidated zein, pure pectin and kaempferol nanoparticles were mixed with potassium bromide and then subjected to FTIR (Nicolet IS5*, Thermo Scientific, CN) analysis scanning from 500 to 4,000 cm^{-1}.

2.3.5. Kaempferol loading efficiency determination

The kaempferol content was determined by a UV spectrometer (UV-1800, SHIMADZU, Japan) as described by Yan et al. (2021). Briefly, samples were prepared in dimethyl sulfoxide (DMSO) at 1mg/mL and measured at 370nm using a UV spectrophotometer. The kaempferol concentration (C_k) was calculated by using a standard curve of kaempferol from 0 to 10μg/mL. The following equations were used to calculated particle yield (PY) and kaempferol loading efficiency (LE):

$$\mathrm{PY} = \frac{Mp}{Mt} \times 100\%$$

$$\mathrm{LE} = \frac{Mkp}{Mkt} \times 100\%$$

Mp: mass of the freeze dried particles; Mt: the total mass used to fabricate the particles; Mkp: mass of kaempferol existed in the nanoparticles; Mkt: the total mass of kaempferol added to prepare the nanoparticles.

2.4. Determination of the stability of nanoparticle dispersions

Kaempferol nanoparticles were subjected to a series of pH values, heat treatments and salt concentrations to study the stability of the nanoparticles including particle size, zeta-potentials and PDI as describe above.

2.4.1. pH

HCl or NaOH solutions (0.1M) were used to change the pH of nanoparticles (1 mg/mL) from 2.0 to 7.5.

2.4.2. Heating

The temperature of Kaempferol nanoparticle dispersions (1 mg/mL) were increased to 80 °C and kept for 0, 10, 20, 30 and 60 min, respectively.

2.4.3. Salt addition

Sodium chloride was dissolved into kaempferol nanoparticle dispersions (1 mg/mL) to form a concentration of 0, 10, 20, and 50 mM solution respectively. After each of these treatments, the overall appearances of the nanoparticle dispersions were recorded by taking a photograph using a digital camera (Cannon EOS R8, Japan). The mean diameter, PDI and zeta-potentials of the particles were determined by dynamic light scattering and particle electrophoresis as described above.

2.5. Antioxidant activity measurements

Antioxidant activity was evaluated by 2,2-diphenyl-1-picrylhydrazyl ($DPPH^{\bullet}$) and 2,2′-azino-bis(3-ethylbenzothiazoline-6-sulfonic acid ($ABTS^{\bullet+}$) free radical scavenging assays (Huang et al., 2017) as described by Liang et al. (2021). Briefly, kaempferol nanoparticle dispersion was incubated with DPPH ethanol solution in the dark for 30 min before measuring absorbance at 517 nm. L-ascorbic acid was used in this experiment as a control for $DPPH^{\bullet}$ scavenging activity. In another experiment, ABTS stock solution was mixed with an potassium persulfate (1/1, v/v) to create the $ABTS^{\bullet+}$ solution. Kaempferol dispersions or other test samples were then added and measured absorbance at 734nm. Free or encapsulated was dispersed in deionized water. The free radical scavenging activity was calculated as follows:

$$\text{Scavenging effect (\%)} = \frac{A_0 - A_s}{A_0} \times 100\%$$

A_0: absorbance of the untreated free radical solution of DPPH or ABTS; As: absorbance of test samples. The concentration for 50% of the scavenging activity (SC_{50}) was calculated by the equation of plotting various sample concentrations against scavenging percentages.

2.6. Simulated gastrointestinal digestion

A simulated gastrointestinal digestion was performed to investigate the evolves of kaempferol nanoparticles in gastrointestinal tract as previously described (Liang et al., 2021).

Gastric phase: briefly samples were treated by pepsin for 2 h in simulated gastric fluids at pH 2.5. This gastric phase was terminated by neutralizing the mixture's pH to 7.0.

Intestine phase: briefly the above fluids were then treated by bile salts and pancreatin at pH 7.0 for 4 h. This intestine phase was terminated by increasing temperature of the mixture to 90 °C and held for 5 min.

Bioaccessibility: The released kaempferol content was determined as describe above. The in vitro bioaccessibility of kaempfeol was calculated as follows:

$$\text{Released (\%)} = \frac{\text{Kaempferol realeased in GI fluids}}{\text{Kaempferol before digestion}} \times 100\%.$$

2.7. In vitro antioxidant capacities of kaempferol after digestion

2.7.1. DPPH scavenging activity assay

DPPH scavenging activity was determined as described in section 2.5. DPPH scavenging activity was converted into the Trolox equivalent antioxidant capacity based on dry weight (μmol TE/g DW) using a standard curve of Trolox solutions. The antioxidant

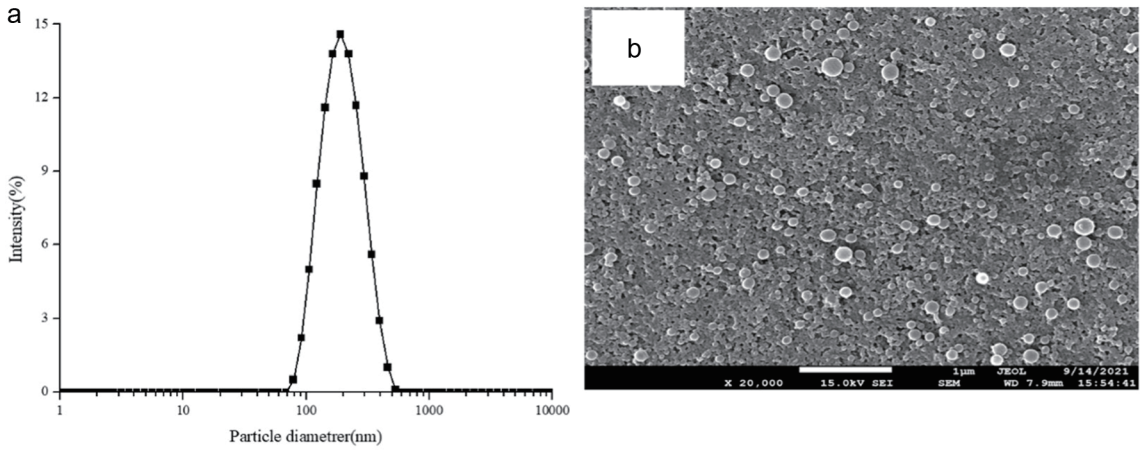

Figure 1. Particle size distribution (a) and SEM image (b) of biopolymer nanoparticles loaded with kaempferol (the pectin concentration in the nanoparticles was 0.1% w/v, while the zein-to-kaempferol ratio was 14:1)

capacity of gastrointestinal fluids was also determined and deducted from the values of test samples.

2.7.2. Oxygen radical absorbance capacity (ORAC) assay

The ORAC assay refers to previous reports by Huang et al. (2002). The degree of change in fluorescence intensity of fluorescein caused by free radicals indicates the activity of the tested antioxidant to inhibit free radicals. The description is as follows: Add 20 μL of samples or Trolox standard (TE, 6.25-50 μM) diluted in 75mM phosphate buffer saline (pH = 7.4) to a 96-well black bottom permeable microtiter plate), add 200μL of fluorescent work (sodium fluorescein, 0.96 μM) to the microplate, and incubate at 37°C in the dark for 20min. After that, 20μL of free radical inducer (2,2′-Azobis(2-amidinopropane) dihydrochloride (ABAP), 119.4 mM) was quickly added to each well, and the quenching intensity of the fluorescence signal of 35 cycles for a total of 150 min was continuously measured in the multifunctional microplate reader (Synergy H1, BioTek, USA). The reaction was 37 °C measurement, fluorescence excitation wavelength and emission wavelength are 485 nm and 535 nm respectively. According to the area under the fluorescence quenching curve (AUC) minus the blank control under the action of antioxidants AUC and TE standard concentration-AUC effect curve, calculated ORAC value of the samples, the data is expressed as: μmol TE/g DW.

2.8. Statistical analysis

Each experiment was carried out in triplicates. Data was represented as mean ± standard deviation and processed by SPSS software (version 13.0, SPSS Inc.). Comparison was analyzed by one-way ANOVA with the Fisher's least significant difference (LSD) test or Dunnett's T3 test. The result was regarded as statistically significant when p-value was less than 0.05.

3. Results and discussion

3.1. Particle yield, loading efficiency and particle properties

Figure 1a indicated that nanoparticle formed a narrow unimodal distribution. At the same time, Table 1 shows the mean size, PDI and the zeta-potential of the nanoparticle was 158.30 ± 1.57 nm, 0.242, -37.6 ± 1.08 mV, respectively. These results suggested that the kaempferol nanoparticles prepared in this study had small size with relatively evenly spread diameter and was negatively charged. Also, the yield of nanoparticle was 99.55% ± 0.33%, kaempferol loading efficiency reached 89.54% ± 5.30%, and the kaempferol loading capacity was 6.52%.

3.2. Particle morphology

SEM was used to study the morphology of the nanoparticle as shown in Figure 1b. The nanoparticle showed a spherical structure with a diameter of ~100 nm, which agreed well with the results from Section 3.1.

3.3. Nanoparticle stability

The effects of pH on Z10-kae-pectin nanoparticles were studied in this experiment (Figure S1). The native pH of the nanoparticle

Table 1. The kaempferol loading efficiency, particle yield, diameter, PDI and zeta-potential of Z10-kae-pectin nanoparticles (n = 3)

Sample	Zein:Kae	Theoretical kaempferol content (%)	Determined kaempferol content (%)	Particle yield (%)	Kaempferol loading efficiency (%)	Particle diameter (nm)	PDI	Zeta potential (mV)
Z10-kae-pectin nanoparticle	14:1	6.52	5.04 ± 0.003[a]	99.55 ± 0.33[a]	89.54 ± 5.30[a]	158.30 ± 1.57[a]	0.242 ± 0.031[a]	-37.60 ± 1.08[a]

Different letters above the bar indicate significant differences between similar sample types with different concentrations (n = 3). PDI: polydispersity index.

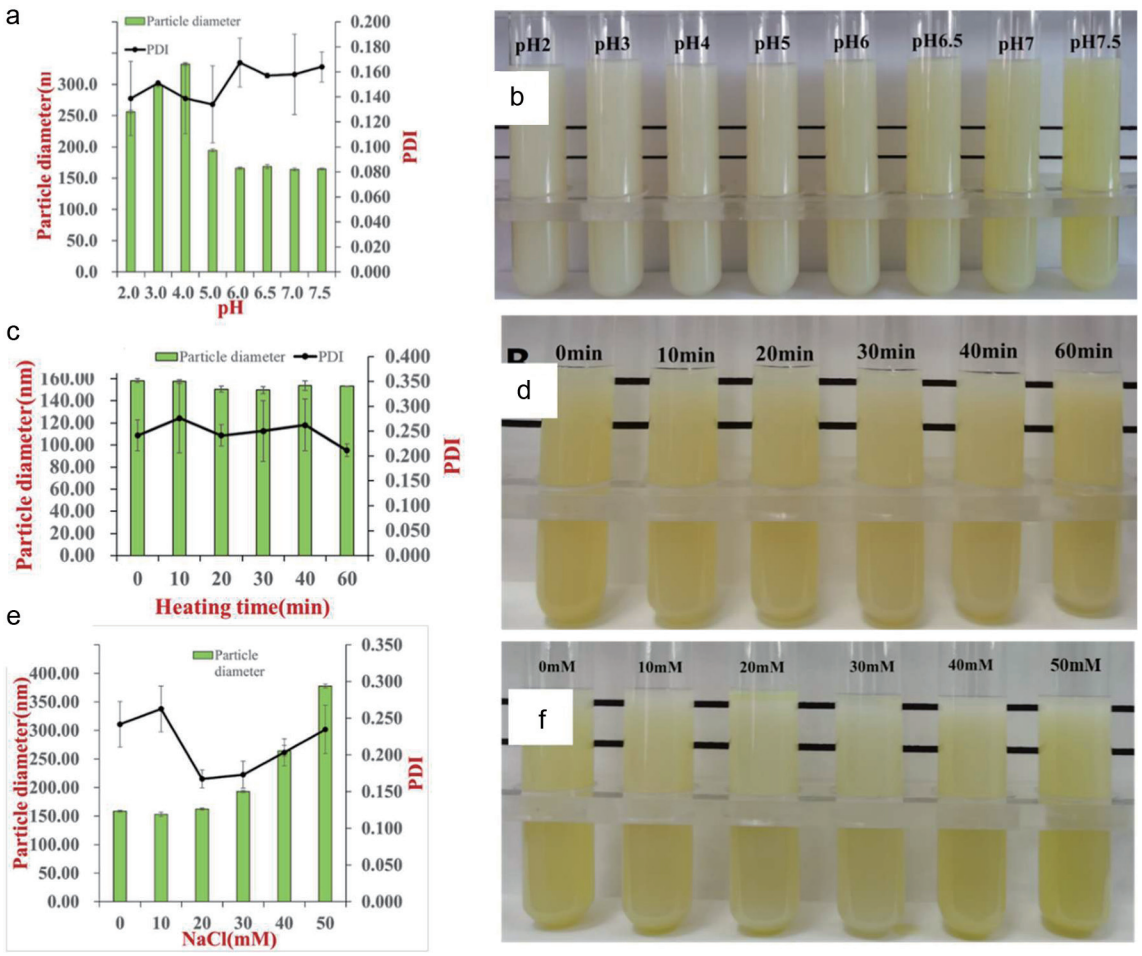

Figure 2. Effect of pH (a, b), heating time (c, d) and NaCl (e, f) on particle size and PDI and the apparent stability of Kae in nanoparticles.

preparations was 6.1, which was first adjusted to 7.5 and then decreased to 2.0. The dispersions were clear and colorless at pH 7.5 but gradually became cloudy at pH 2.0; however, no precipitation occurred during the experiment (Figure 2b). Considering the particle diameter increased from 164.03 ± 4.67 nm to 332.43 ± 20.88 nm, the above observation at different pHs may be a result of increased particle size (Figure 2a). The polydispersity (PDI<0.167) remained relatively low across the entire pH range studied, which accounts for their good resistance to sedimentation during storage.

Precipitation of nanoparticles created by zein protein tended to occur around pH 6.2, the isoelectric point (Li and Yao, 2020) of zein (Shukla and Cheryan, 2001), as the negative charge is almost neutralized and hydrophobicity will cause aggregation (Hu and McClements, 2014). However, pectin molecules adhered onto the surface may prevent zein nanoparticles from precipitation. Pectin is a natural polycarboxylic acid polymer. The electrostatic repulsion from its side chains keeps the nanoparticles solubilized at the PI of zein protein (Huang et al., 2019).

The stability of nanoparticle preparations under heat treatments (80 ºC for 0, 10, 20, 30, 60 min) was also investigated. With the extension of heating time, the appearance of nanoparticles becomes slightly turbid (Figure 2d). Mean particle diameter and PDI did not show significant changes when the nanoparticle dispersions were heated at 80 °C for up to 60 min. The particle size is between 149.73 ± 5.66 nm and 158.30 ± 3.09 nm, and the PDI is between 0.211-0.277 (Figure 2c). This result suggests that the Z10-kae-pectin nanoparticles prepared in this study were stable under heat treatment.

In addition, the dispersions became more turbid at high salt concentrations (50mM NaCl) (Figure 2f). As the concentration of sodium chloride increases, the particle size gradually increases (153.00 - 377.80 nm), but the PDI is less than 0.263 (Figure 2e), indicating that the particle distribution is relatively uniform. From the above results, Z10-pectin-kaempferol (kae) nanoparticle has better pH, heat and salt stability, hence it was selected for subsequent experiments.

3.4. FTIR analysis

The FTIR spectroscopy was used to study the possible chemical changes during the formation of zein-kaempferol particles (Figure 3a). The patterns in the spectra represent certain functional groups of the analyzed molecules. In the spectrum of pectin, the band at 3,437 cm^{-1} is the stretching vibration of –OH groups (Zhao et al., 2019), the stretching vibrations of -CH (Chai et al., 2018) was attributed to the peak at 2,939 cm^{-1}, while the relatively strong peak at 1,745 cm^{-1} was originated from the -C=O group stretching vibrations (Dong et al., 2019), and the band located at 1,099 cm^{-1} was caused by the stretching vibration of C-O (Kang et al., 2019).

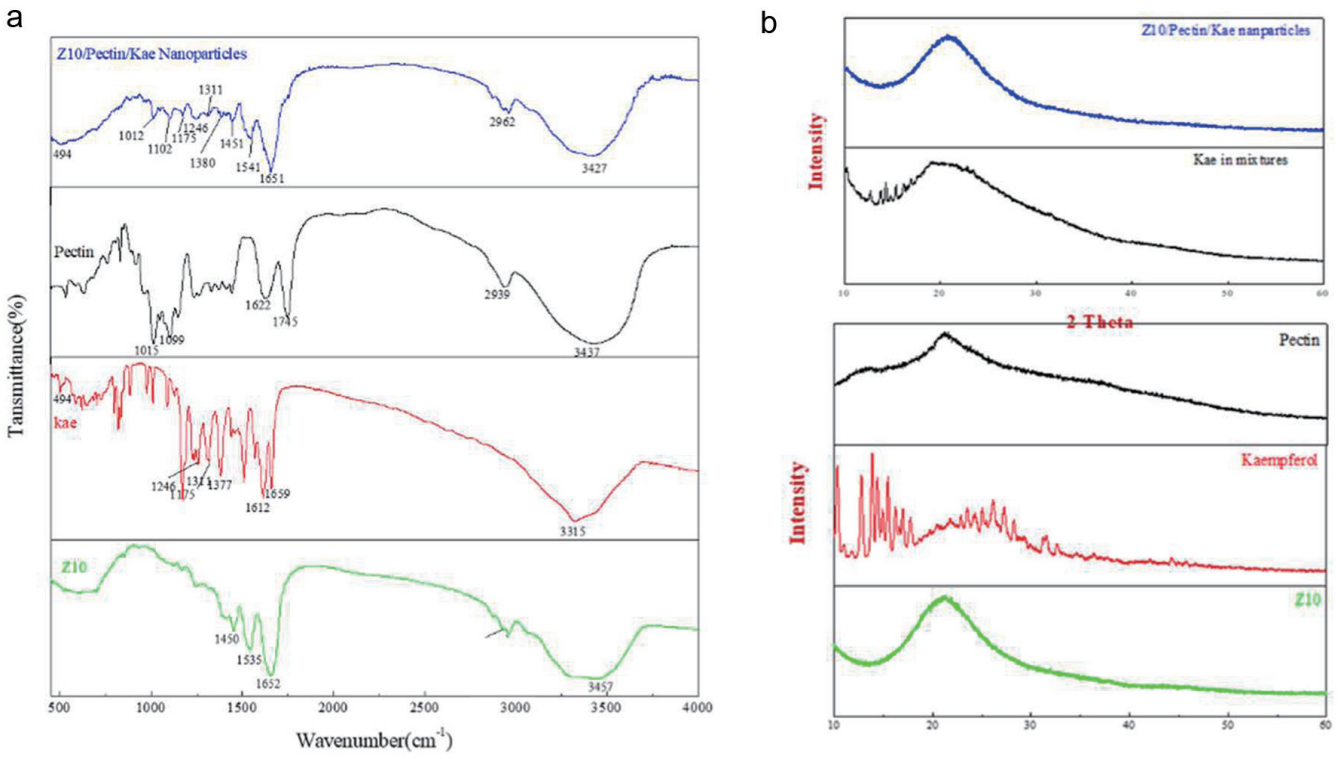

Figure 3. Fourier transform infrared spectroscopy (FTIR) (a) and XRD spectra (b) of kaempferol, zein, pectin and kaempferol-loaded zein nanoparticles.

As a natural flavonoid, four hydroxyl groups are incorporated in the structure of kaempferol, acting as hydrogen-bond donor sites. Meanwhile, the C ring possess the 4-oxo group, which can form up to two intramolecular hydrogen bonds (Trendafilova et al., 2021). The hydroxylated B-ring, and the double bonds C_2=C_3 and C=O in C-ring, are the important structural characteristic of kaempferol, remarkably associated with the stability of the radicals in flavonoids (Heim et al., 2002). The pattern in the region 1,700–1,000 cm^{-1} is preponderant in the IR spectrum of kaempferol. The bands below 1,000 cm^{-1} are observed as out-of-plane vibrations, which perform lower intensities (Baranović and Šegota, 2018; Machado et al., 2013). For zein, 3,457 cm^{-1} (N–H stretching), 2,958 cm^{-1} and 2,932 cm^{-1} (C–H stretching) (Shinde et al., 2020), 1,652 cm^{-1} (Amide I, linked to C–O/hydrogen bonding), 1,535 cm^{-1} (Amide II, linked to CN stretching and NH bending modes), 1,450 cm^{-1} (CH_2 bending) (Guo et al., 2021) are the main absorption bands.

For the zein-pectin-kae nanoparticles, the peaks of the hydroxyl groups shifted to 3,427 cm^{-1}, indicating the hydrogen bond was formed among zein, kaempferol, and pectin. The peaks of C–O vibration in pectin shifted from 1,099 to 1,102 cm^{-1}, and the peaks shifted from 1,535 to 1,541 cm^{-1} are associated with the CN stretching and NH bending of zein, which indicate that electrostatic interactions were significant during the formation of zein-pectin-kae nanoparticles (Smruthi et al., 2022; Wang et al., 2021). Importantly, the dominant characteristic peaks of kaempferol were observed at 1,311 cm^{-1}, 1,246 cm^{-1}, 1,175 cm^{-1}, and 494 cm^{-1}, but disappear in the spectra of loaded nanoparticles, which demonstrated kaempferol was successfully entrapped within the nanoparticle core. This results are consistent with previous findings reported by Hu et al. (2015), reporting that the characteristic peaks of curcumin did not appear when encapsulated in zein nanoparticles form.

3.5. X-ray diffraction analysis

The XRD patterns of pectin, deamidated zein and kaempferol in nanoparticles compared with free form kaempferol, were performed in Figure 3b. Diffraction peaks were observed for pure kaempferol at 2θ angles of 10.39°, 12.63°, 15.40°, 23.06°, 24.24° and 27.28°, indicating that it was in a crystalline form (Ilk et al., 2017). The peaks of physical mixture performed numbers of 10.30, 12.74, 13.73, 14.35, 15.34, 16.25 and 17.05 at 2θ angles, which also confirmed a crystalline form. Due to the relatively low concentration of kaempferol in the physical mixture (5.63%, w/w), other characteristic peaks were too weak to be observable. More relevantly, after nanoparticle construction, an amorphous structure of kaempferol was observed, while the crystalline peaks disappeared.

3.6. In vitro antioxidant capacity of kaempferol in nanoparticles

Kaempferol is a natural flavonol that has poor water solubility but strong antioxidant activity. In this section, the antioxidant activity of kaempferol with and without encapsulation was studied by using $DPPH^{\bullet}$ and $ABTS^{\bullet+}$scavenging assays.

Ascorbic acid is a natural antioxidant and often used as a positive control in antioxidant assays. As shown in Figure 4a, the free radical scavenging activity of ascorbic acid increased to 85.42 ± 0.07% with increasing concentration to 10 μg/mL. For kaempferol ethanol solution, the scavenging percentage reached 78.85% ± 0.21%. The $DPPH^{\bullet}$ scavenging activity of encapsulated kaempferol was close to that of ascorbic acid and kaempferol alone, reaching 75.46% ± 0.59% at 10 μg/mL. In terms of SC_{50}, ascorbic acid, encapsulated kaempferol, and kaempferol alone were 4.43

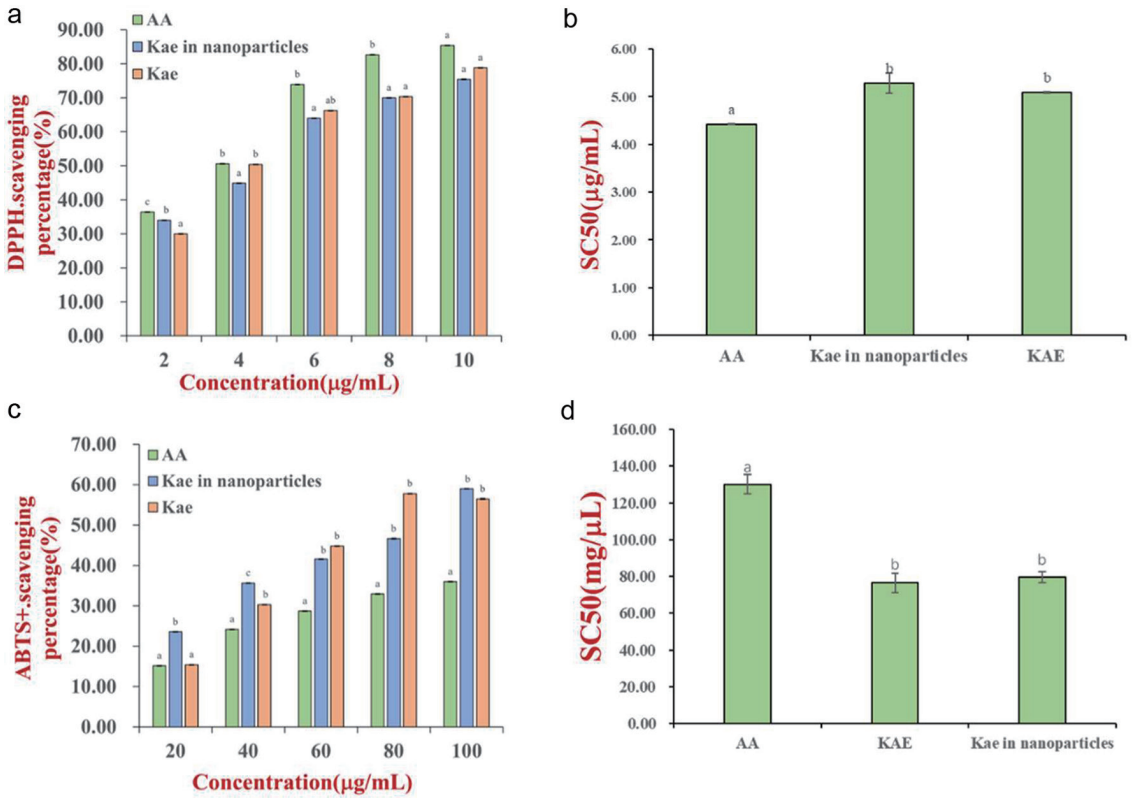

Figure 4. The radical scavenging activity (a, c) and scavenging SC_{50} (b, d) of kaempferol-loaded nanoparticles compared with free form and ascorbic acid (n = 3).

± 0.61, 5.28 ± 0.57, and 5.09 ± 0.55 μg/mL, respectively (Figure 4b). Encapsulated kaempferol was similar to kaempferol alone at scavenging DPPH• radicals (p>0.05). This suggested encapsulated kaempferol has similar antioxidant activity with free form of kaempferol.

To confirm the above results and provide more information, $ABTS^{•+}$ scavenging assay was also used to analyze the antioxidant activity of the kaempferol nanoparticles. The $ABTS^{•+}$ scavenging activity of encapsulated kaempferol and kaempferol alone exhibited a dose dependent relationship, achieving 58.98% ± 0.35% and 56.44% ± 1.01% at 100 μg/mL, respectively compared with that of ascorbic acid was 36.65% at the same concentration (Figure 4c). The SC_{50} values of the ascorbic acid, encapsulated kaempferol and kaempferol ethanol solution were 130.18 ± 5.92, 79.64 ± 1.04 and 76.61 ± 1.48 μg/mL, respectively (Figure 4d). These results suggested that the radical scavenging activity of kaempferol was comparable with encapsulated kaempferol but significantly higher than that of ascorbic acid in this experiment. A possible explanation for this higher activity than ascorbic acid is that the negatively charged kaempferol nanoparticles may appeal the positively charged ABTS• and DPPH•, and thus accelerate the antioxidant reaction between these free radicals and kaempferol.

3.7. Kaempferol release under simulated digestion conditions

The evolve of kaempferol nanoparticles under simulated digestion was investigated (Figure 5). The bioaccessibility in the GI tract is critical for polyphenols as it will affect the bioactivities of these compounds. This experiment was thus designed to study the re-

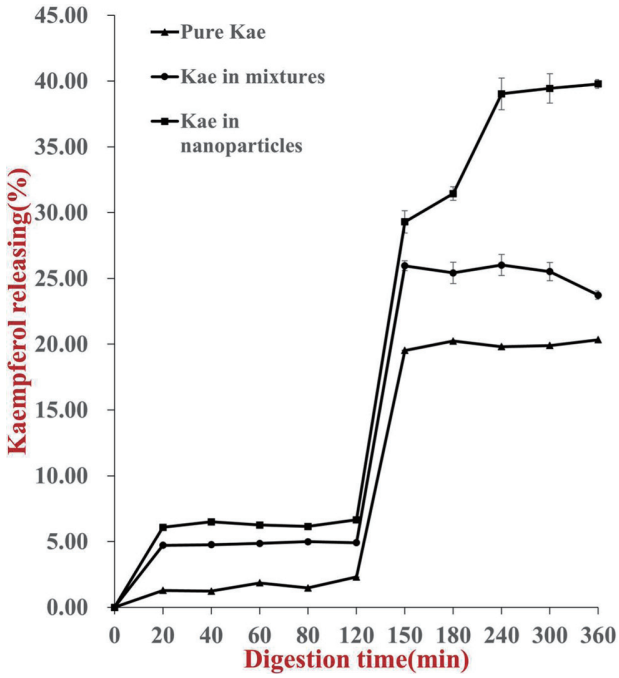

Figure 5. Releasing percentage of nanoparticle encapsulated kaempferol (kae), kaempferol mixture (with the same compositions) and pure kaempferol (crystalline form) during incubated in stimulated gastric and small intestinal fluids (n = 3).

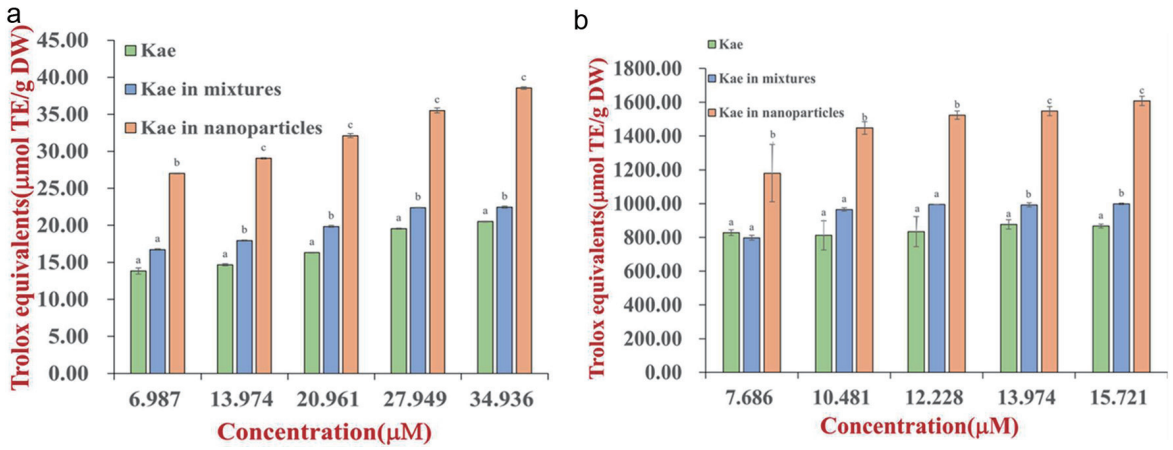

Figure 6. Radical scavenging capacity (a) and Oxygen radical absorbance capacity (b) of different kaempferol formulations after 120 min stimulated gastric digestion and 240 min small intestinal digestion prior to analysis, expressed as Trolox equivalent values, (n = 3).

lease process of kaempferol from the nanoparticles during a simulated digestion.

All the kaempferol nanoparticles experienced a rapid release of kaempferol for the first 20 min of gastric digestion, and then the release rate was lowered to a relatively constant level for the remaining gastric phase. The first 20 min digestion resulted 1.28% pure kaempferol and 4.71% kaempferol in the physical mixtures released from the formulation. The released kaempferol was at a low concentration which was probably due to the fact that it was crystallized (as shown in Figure 3b), and thus resistant to gastric digestion. In the next intestinal stage, the release of kaempferol from both the pure crystal form and the physical mixtures was significantly elevated; however, more kaempferol was released from the physical mixture than from the crystal form. One possible explanation for such observation is that bile salts and zein hydrolysates produced in the intestinal stage may assist the solubilization of kaempferol (Yao et al., 2018). At the end of the experiment, the released kaempferol experienced a decrease, which may be a result from recrystallization or chemical degradation (Davidov-Pardo et al., 2015).

The percentage of kaempferol released from the composite nanoparticles increased steadily during the gastric stage, reaching around 6.66% by the end, which was higher than that for the pure kaempferol or the physical mixtures. The final bioaccessibility of the kaempferol encapsulated within the composite nanoparticles was 39.78% after the intestinal phase, which was significantly higher than that for the pure kaempferol (20.34%) and physical mixtures (23.73%). These results supported that encapsulation with zein protein could improve the bioaccessibility of kaempferol during simulated digestion. These findings can be attributed to the formation of amorphous polyphenols during encapsulation which revealed faster release rate and better solubilization than crystalline polyphenols during digestion (Yao et al., 2018). The protein coating of the nanoparticles can be readily hydrolyzed by pancreatin and then the amorphous kaempferol was released and solubilized by bile salts and peptides.

3.8. In vitro antioxidant capacity of digested kaempferol formulation

Digestion will often jeopardize the structure integrity of bioactive compounds and therefore negatively affect their health benefits. It is critical to re-assess the antioxidant activities of kaempferol nanoparticles after digestion. In this experiment, the antioxidant capacities of digested kaempferol nanoparticles were analyzed by DPPH scavenging capacity assay (Figure 6a) and oxygen radical absorbance capacity assay (Figure 6b). As shown in Figure 6a, with the increase of kaempferol content in the digestive juice, the DPPH scavenging capacity of kaempferol, kaempferol mixtures and kaempferol nanoparticles all show an upward trend, but the kaempferol nanoparticles have the strongest scavenging ability, and the range is 27.00 ± 0.06 to 38.55 ± 0.17 μmol TE/g DW. Similarly, Figure 6b shows the ORAC of different forms of kaempferol digestive fluids. With the increase of kaempferol content, the ORAC value of kaempferol alone does not change much, while kaempferol mixtures and kaempferol nanoparticles basically show an upward trend. The ORAC value of kaempferol nanoparticles is between 1,180.13 ± 170.18 and 1,607.64 ± 27.73. Overall, these results indicate that the antioxidant properties of kaempferol-loaded nanoparticles were enhanced after simulated digestion. This observation can be explained by faster release and better solubility of encapsulated kaempferol during digestion as discussed in the previous section. It is noteworthy that, after digestion the concentration of kaempferol from physical mixtures was similar to that from kaempferol powder, but the physical mixtures possessed a higher antioxidant capacity. The peptides from zein protein digests may also contribute to the overall antioxidant activity (Yan et al., 2021).

4. Conclusion

This study introduced a method to produce kaempferol-loaded complex nanoparticles with mean diameter of 158.3 nm. The nanoparticle preparations possessed a high yield (99%), encapsulation efficiency (89%), and kaempferol content (6.5%) than previous publications. The kaempferol nanoparticles were relatively stable under a wide range of pH, concentrations of salts, and heating conditions without aggregation. Such properties are favorable for its potential uses in a broad range of nutraceuticals. The kaempferol-loaded nanoparticles interacted with each other through hydrogen bonding and electrostatic interactions. Most of the kaempferol nanoparticles passed through gastric digestion and were released during the intestinal phase. The antioxidant activity of encapsulated kaempferol was comparable to that of free kaempferol, while the bioaccessibility of encapsulated kaempferol was even higher

than that of free kaempferol *in vitro* experiments. The above results suggest that complex nanoparticles could be an effective delivery system for kaempferol or other polyphenols. However, in *vivo* animal and human studies are needed to prove the efficacy of the kaempferol-loaded delivery system under realistic conditions. Meanwhile, the antioxidant activity of kaempferol nanoparticles should be further verified.

Acknowledgments

The animal experiment center of Guangdong Pharmaceutical University is gratefully acknowledged.

Data availability

Data available on request from the authors. The data that support the findings of this study are available from the corresponding author, upon reasonable request.

Funding

The financial support of the Education department of Guangdong Province (No 2021KTSCX050), and the Traditional Chinese Medicine Bureau of Guangdong Province (No 20221217) are appreciated and acknowledged. This work is also supported by Yunfu Traditional Chinese Medicine Innovation Team Project (No KTP20240943) and the Research Group of Functional Foods Development for Specific Populations (No 2024ZZ12).

Conflict of interest

The authors declare that they have no known competing financial interests or personal relationships that could have appeared to influence the work reported in this paper.

Author contributions

Xiaoyun Rong: Writing – original draft; Ruixue Guo & Kun Hu, design the experiment and guide all the operation as well as revise the manuscript; Jiandong Ren and Xinbo Guo, revises the draft; ; Chao Huang, help Rong to analysis the data; Fenglin Song, participated in the simulated experiments; and Yongguang Bi analyzed the Raw data.

Supplementary material

Figure S1. The effect of pH on the apparent stability of nanoparticles.

References

Baranović, G., and Šegota, S. (2018). Infrared spectroscopy of flavones and flavonols. Reexamination of the hydroxyl and carbonyl vibrations in relation to the interactions of flavonoids with membrane lipids. Spectrochim. Acta A Mol. Biomol. Spectrosc. 192: 473–486.

Cabra, V., Arreguin, R., Vazquez-Duhalt, R., and Farres, A. (2007). Effect of alkaline deamidation on the structure, surface hydrophobicity, and emulsifying properties of the Z19 alpha-zein. J. Agric. Food Chem. 55(2): 439–445.

Chai, W., Huang, Y., Peng, W., Han, G., Cao, Y., and Liu, J. (2018). Enhanced separation of pyrite from high-sulfur bauxite using 2-mercaptobenzimidazole as chelate collector: Flotation optimization and interaction mechanisms. Miner. Eng. 129: 93–101.

Chen, A.Y., and Chen, Y.C. (2013). A review of the dietary flavonoid, kaempferol on human health and cancer chemoprevention. Food Chem. 138(4): 2099–2107.

Davidov-Pardo, G., Pérez-Ciordia, S., Marín-Arroyo, M.A.R., and McClements, D.J. (2015). Improving Resveratrol Bioaccessibility Using Biopolymer Nanoparticles and Complexes: Impact of Protein–Carbohydrate Maillard Conjugation. J. Agric. Food Chem. 63(15): 3915–3923.

Dong, L., Jiao, F., Qin, W., and Liu, W. (2019). Selective flotation of scheelite from calcite using xanthan gum as depressant. Miner. Eng. 138: 14–23.

Ghosh, A., Khanam, N., and Nath, D. (2024). Solid lipid nanoparticle: A potent vehicle of the kaempferol for brain delivery through the blood-brain barrier in the focal cerebral ischemic rat. Chem.-Biol. Interact. 397(000): 13.

Guo, Y., Bao, Y.-H., Sun, K.-F., Chang, C., and Liu, W.-F. (2021). Effects of covalent interactions and gel characteristics on soy protein-tannic acid conjugates prepared under alkaline conditions. Food Hydrocolloids 112: 106293.

Heim, K.E., Tagliaferro, A.R., and Bobilya, D.J. (2002). Flavonoid antioxidants: chemistry, metabolism and structure-activity relationships. J. Nutr. Biochem. 13(10): 572–584.

Hu, K., and McClements, D.J. (2014). Fabrication of surfactant-stabilized zein nanoparticles: A pH modulated antisolvent precipitation method. Food Res. Int. 64: 329–335.

Hu, K., Huang, X., Gao, Y., Huang, X., Xiao, H., and McClements, D.J. (2015). Core–shell biopolymer nanoparticle delivery systems: Synthesis and characterization of curcumin fortified zein–pectin nanoparticles. Food Chem. 182: 275–281.

Huang, D., Ou, B., Hampsch-Woodill, M., Flanagan, J.A., and Prior, R.L. (2002). High-throughput assay of oxygen radical absorbance capacity (ORAC) using a multichannel liquid handling system coupled with a microplate fluorescence reader in 96-well format. J. Agric. Food Chem. 50(16): 4437.

Huang, X., Dai, Y., Cai, J., Zhong, N., Xiao, H., Mcclements, D.J., and Hu, K. (2017). Resveratrol encapsulation in core-shell biopolymer nanoparticles: Impact on antioxidant and anticancer activities. Food Hydrocolloids 64(mar.): 157–165.

Huang, X., Liu, Y., Zou, Y., Liang, X., Peng, Y., McClements, D.J., and Hu, K. (2019). Encapsulation of resveratrol in zein/pectin core-shell nanoparticles: Stability, bioaccessibility, and antioxidant capacity after simulated gastrointestinal digestion. Food Hydrocolloids 93: 261–269.

Ilk, S., Sağlam, N., Özgen, M., and Korkusuz, F. (2017). Chitosan nanoparticles enhances the anti-quorum sensing activity of kaempferol. Int. J. Biol. Macromol. 94: 653–662.

Imran, M., Rauf, A., and Imran, A. (2019). Chemo-preventive and therapeutic effect of the dietary flavonoid kaempferol: A comprehensive review. Phytother. Res. 33(2): 263–275.

Kaffash, M., Tolou-Shikhzadeh-Yazdi, S., Soleimani, S., Hoseinpoor, S., Saberi, M.R., and Chamani, J. (2024). Spectroscopy and molecular simulation on the interaction of Nano-Kaempferol prepared by oil-in-water with two carrier proteins: An investigation of protein-protein interaction. Spectrochim. Acta A Mol. Biomol. Spectrosc. 309: 123815.

Kang, M., Oderinde, O., Liu, S., Huang, Q., Ma, W., Yao, F., and Fu, G. (2019). Characterization of Xanthan gum-based hydrogel with Fe3+ ions coordination and its reversible sol-gel conversion. Carbohydr. Polym. 203: 139–147.

Kasaai, M.R. (2018). Zein and zein -based nano-materials for food and nutrition applications: A review. Trends Food Sci. Technol. 79: 184–197.

Kashyap, D., Sharma, A., Tuli, H.S., Sak, K., Punia, S., and Mukherjee, T.K. (2017). Kaempferol – A dietary anticancer molecule with multiple mechanisms of action: Recent trends and advancements. J. Funct.

Foods 30: 203–219.
Li, L., and Yao, P. (2020). High dispersity, stability and bioaccessibility of curcumin by assembling with deamidated zein peptide. Food Chem. 319: 126577.
Li, Z., Jiang, H., Xu, C., and Gu, L. (2015). A review: Using nanoparticles to enhance absorption and bioavailability of phenolic phytochemicals. Food Hydrocolloids 43: 153–164.
Liang, X., Cao, K., Li, W., Li, X., McClements, D.J., and Hu, K. (2021). Tannic acid-fortified zein-pectin nanoparticles: Stability, properties, antioxidant activity, and in vitro digestion. Food Res. Int. 145: 110425.
Machado, N.F.L., Batista de Carvalho, L.A.E., Otero, J.C., and Marques, M.P.M. (2013). A conformational study of hydroxyflavones by vibrational spectroscopy coupled to DFT calculations. Spectrochim. Acta A Mol. Biomol. Spectrosc. 109: 116–124.
Qu, Z., Chen, G., Yang, T., Li, S., and Chen, Y. (2024). Mechanisms underlying the formation of non-thermal deamidated zein via synergistic treatment of cold plasma with acid: improved foam performance. Food Hydrocolloids 146: 109195.
Rajendran, P., Rengarajan, T., Nandakumar, N., Palaniswami, R., Nishigaki, Y., and Nishigaki, I. (2014). Kaempferol, a potential cytostatic and cure for inflammatory disorders. Eur. J. Med. Chem. 86: 103–112.
Shinde, P., Agraval, H., Srivastav, A.K., Yadav, U.C.S., and Kumar, U. (2020). Physico-chemical characterization of carvacrol loaded zein nanoparticles for enhanced anticancer activity and investigation of molecular interactions between them by molecular docking. Int. J. Pharm. 588: 119795.
Shukla, R., and Cheryan, M. (2001). Zein: the industrial protein from corn. Ind. Crops Prod. 13(3): 171–192.
Silva dos Santos, J., Goncalves Cirino, J.P., de Oliveira Carvalho, P., and Ortega, M.M. (2021). The pharmacological action of kaempferol in central nervous system diseases: a review. Front. Pharmacol. 11: 565700.
Smruthi, M.R., Nallamuthu, I., and Anand, T. (2022). A comparative study of optimized naringenin nanoformulations using nano-carriers (PLA/PVA and zein/pectin) for improvement of bioavailability. Food Chem. 369: 130950.
Subbaraj, G.K., Masoodi, T., Yasam, S.K., Chandrashekar, K., Kulanthaivel, L., Shaik, N.A., Hashem, S., Akil, A.S.A., and Bhat, A.A. (2023). Anti-angiogenic effect of nano-formulated water soluble kaempferol and combretastatin in an in vivo chick chorioallantoic membrane model and HUVEC cells. Biomed. Pharmacother. 163(000): 11.
Tian, Q., Chen, F., Tan, X., Zhao, G., and Ye, F. (2019). Preparation and physicochemical properties of sulforaphane-encapsulated zein aqueous nano-dispersions. Food Ferment. Ind. 045(001): 121–127.
Trendafilova, I., Lazarova, H., Chimshirova, R., Trusheva, B., Koseva, N., and Popova, M. (2021). Novel kaempferol delivery systems based on Mg-containing MCM-41 mesoporous silicas. J. Solid State Chem.` 301: 122323.
Türker, D.A. (2025). Influence of charged polysaccharides and zein nanoparticles on the interfacial and emulsification properties of Pickering emulsions. Food Hydrocolloids 161: 110887.
Wang, L., Huang, D., Li, K., Dai, Y., Song, A., He, L., and & Wang, L. (2024b). Fabrication, characterization and mechanistic exploration of zein/pectin binary nanocomplex by a one-step and organic solvent free technique. LWT 204: 116349.
Wang, L., Huang, X., Cao, X., Zhou, F., Liu, B., Wei, S., Liu, X., Yang, X., and Yin, S. (2024a). Confining the Growth of AgNPs onto Epigallocatechin Gallate-Decorated Zein Nanoparticles for Constructing Potent Protein-Based Antibacterial Nanocomposites. J. Agric. Food Chem. 72(9): 4928–4938.
Wang, X., Li, M., Liu, F., Peng, F., Li, F., Lou, X., Jin, Y., Wang, J., and Xu, H. (2021). Fabrication and characterization of zein-tea polyphenols-pectin ternary complex nanoparticles as an effective hyperoside delivery system: Formation mechanism, physicochemical stability, and in vitro release property. Food Chem. 364: 130335.
Wang, X., Yang, Y., An, Y., and Fang, G. (2019). The mechanism of anticancer action and potential clinical use of kaempferol in the treatment of breast cancer. Biomed. Pharmacother. 117: 109086.
Yan, Z.A., Yi, Q.A., Xr, A., Kc, A., Mc, B., and Kh, A. (2021). Encapsulation of quercetin in biopolymer-coated zein nanoparticles: Formation, stability, antioxidant capacity, and bioaccessibility. Food Hydrocolloids 120: 106980.
Yao, K., Chen, W., Song, F., McClements, D.J., and Hu, K. (2018). Tailoring zein nanoparticle functionality using biopolymer coatings: Impact on curcumin bioaccessibility and antioxidant capacity under simulated gastrointestinal conditions. Food Hydrocolloids 79: 262–272.
Zhang, D., Jiang, F., Ling, J., Ouyang, X.K., and Wang, Y.G. (2021). Delivery of curcumin using a zein-xanthan gum nanocomplex: Fabrication, characterization, and in vitro release properties. Colloids Surf., B 204: 111827.
Zhang, Y., Cui, L., Li, F., Shi, N., Li, C., Yu, X., Chen, Y., and Kong, W. (2016). Design, fabrication and biomedical applications of zein-based nano/micro-carrier systems. Int. J. Pharm. 513(1-2): 191–210.
Zhao, K., Wang, X., Wang, Z., Yan, W., Zhou, X., Xu, L., and Wang, C. (2019). A novel depressant for selective flotation separation of pyrite and pyrophyllite. Appl. Surf. Sci. 487: 9–16.